Appl Biochem Biotechnol (2015) 175:477–488
DOI 10.1007/s12010-014-1290-7

Molecular Characterization and Expression Analyses of an Anthocyanin Synthase Gene from *Magnolia sprengeri* Pamp.

Shou-Guo Shi · Shan-Ju Li · Yong-Xiang Kang · Jian-Jun Liu

Received: 31 May 2014 / Accepted: 7 October 2014 /
Published online: 15 October 2014

Abstract Anthocyanin synthase (ANS), which catalyzes the conversion of colorless leucoanthocyanins into colored anthocyanins, is a key enzyme in the anthocyanin biosynthetic pathway. It plays important roles in plant development and defense. An *ANS* gene designated as *MsANS* was cloned from *Magnolia sprengeri* using rapid amplification of complementary DNA (cDNA) ends technology. The full-length *MsANS* is 1171-bp long and contains a 1080-bp open reading frame encoding a 360 amino acid polypeptide. In a sequence alignment analysis, the deduced MsANS protein showed high identity to ANS proteins from other plants: *Prunus salicina* var. *cordata* (74 % identity), *Ampelopsis grossedentata* (74 % identity), *Pyrus communis* (73 % identity), and *Prunus avium* (73 % identity). A structural analysis showed that MsANS belongs to 2-oxoglutarate (2OG)- and ferrous iron-dependent oxygenase family because it contains three binding sites for 2OG. Real-time quantitative polymerase chain reaction analyses showed that the transcript level of *MsANS* was 26-fold higher in red petals than in white petals. The accumulation of anthocyanins in petals of white, pink, and red *M. sprengeri* flowers was analyzed by HPLC. The main anthocyanin was cyanidin-3-*o*-glucoside chloride, and the red petals contained the highest concentration of this pigment.

Shou-Guo Shi and Shan-Ju Li contributed equally to this work.

Electronic supplementary material The online version of this article (doi:10.1007/s12010-014-1290-7) contains supplementary material, which is available to authorized users.

S.-G. Shi · S.-J. Li
Life Sciences Department, Yuncheng University, Yuncheng 044000 Shanxi, China

S.-G. Shi
e-mail: shishouguo2009@163.com

S.-J. Li
e-mail: lishanju_0@163.com

S.-G. Shi · Y.-X. Kang · J.-J. Liu (✉)
College of Forestry, Northwest A&F University, Yangling, Xian 712100 Shaanxi, China
e-mail: ljj@nwsuaf.edu.cn

Y.-X. Kang
e-mail: yxkang@nwsuaf.edu.cn

Keywords *Magnolia sprengeri* · Anthocyanin synthase · Characterization · Cloning · Gene expression

Introduction

Magnolia sprengeri Pamp. is one of the most valuable medicinal and ornamental plants in the Magnolia family. It is native to the Qinling–Daba Mountains in Shaanxi and Hubei provinces, China [1]. In nature, the flowers of *M. sprengeri* range in color from white to red. Although Chinese magnolias represent a rich genetic resource, there are few reports on important genes in these species. Therefore, research on the mechanisms of coloration of magnolia flowers has practical significance for the protection and reasonable use of these resources.

Anthocyanins are a major group of floral pigments in higher plants. Anthocyanin accumulation is tightly linked to flower development and color change [2]. These compounds have a variety of protective functions against biotic and abiotic stresses [3–7]. Anthocyanins represent an important class of polyphenols that are beneficial for human health. The anthocyanins from many plants have been studied extensively in terms of their antioxidant capacity. They also have other important nutraceutical properties and are associated with the prevention of heart disease and certain cancers [8–11].

There have been several studies on anthocyanin biosynthesis via the flavonoid metabolic pathway during flower development [12–14]. Anthocyanins are biosynthesized from phenylalanine, with the first step catalyzed by phenylalanine ammonia-lyase (PAL). Two groups of genes are important in anthocyanin biosynthesis: structural genes and regulatory genes. The structural genes encode important enzymes in anthocyanin biosynthesis including PAL, chalcone synthase (CHS), flavanone 3-hydroxylase (F3H), dihydroflavonol 4-reductase (DFR), anthocyanin synthase (ANS), and UDP-glucose flavonoid 3-*O*-glucosyltransferase (UFGT) [15–20]. ANS, which catalyzes colorless leucoanthocyanins into colored anthocyanin, is a key enzyme in the late stages of anthocyanin biosynthesis [21]. Cloning and expression analyses of *ANS* genes have shown that increased transcript levels of *ANS* coincide with the timing and location of anthocyanin accumulation [22–25]. The flowers of *M. sprengeri* accumulate anthocyanin; the amount depending on their color. Therefore, to understand the molecular basis of coloration of magnolia flowers, it is important to analyze the structure and expression profile of the *ANS* gene. This information will also be useful for controlling flower color of magnolias via genetic engineering strategies. The regulatory genes involved in anthocyanin biosynthesis include those encoding transcription factors (TFs), which regulate the expression of the biosynthetic genes. The important TFs for anthocyanin biosynthesis are in the MYB, bHLH, and WD40 families [26–31]. The coordinated expressions of structural and regulatory genes lead to anthocyanin accumulation during the color development process.

In this study, we isolated an ANS gene, *MsANS*, from the petals of *M. sprengeri.* We investigated the structure of the gene, determined the amino acid (AA) composition and hydrophobic/hydrophilic regions of the putative protein, and created a three-dimensional model. Using high-performance liquid chromatography (HPLC), we identified the anthocyanin in *M. sprengeri* flowers and determined its contents in petals of white, pink, and red flowers. We also determined the transcript levels of *MsANS* in the petals. These results are useful for understanding the molecular mechanism of anthocyanin synthesis in *M. sprengeri* and provide a basis to improve the flower color of magnolias.

Materials and Methods

Plant Materials

Flowers of four different colors, ranging from white to red, were harvested from approximately 50-year-old trees of *M. sprengeri* from the Qinling–Daba Mountains in March 2012. The petals were detached from the flowers, cleaned, cut into small pieces, and then immediately frozen in liquid nitrogen. The floral tissues were stored at −80 °C until further processing.

RNA Isolation and Reverse Transcription

Total RNA was extracted from the petals of red and white *M. sprengeri* floral tissues using TRIzol Reagent (Invitrogen, Carlsbad, CA, USA) according to the manufacturer's instructions. The purity of all RNA samples was determined from the absorbance ratio of OD260/280, and RNA quality was tested by electrophoresis on a 1 % (*w*/*v*) agarose gel stained with ethidium bromide. The RNA concentration was assessed using a GeneQuant100 spectrophotometer (GE Healthcare, Buckinghamshire, UK) before processing. After isolation, RNA was stored at −80 °C until use.

Cloning of Full-Length cDNA of *MsANS*

Single-stranded cDNAs were synthesized from 5 μg total RNA with an oligo($_{dT}$) primer according to the manufacturer's protocol (PowerScript, Clontech, Palo Alto, CA, USA). After RNaseH treatment, the single-stranded complementary DNA (cDNA) mixture was used as the template for polymerase chain reaction (PCR) amplification of the *MsANS* fragment with the primers pANS1-1: 5′-GCTTGAGTGGGAGGATTATTT-3′ and pANS1-2: 5′-CTCT TTAGGAGG CTCGCAGA-3′. The PCR cycling conditions were as follows: denaturation at 94 °C for 5 min followed by 36 cycles of amplification (94 °C for 1 m, 55 °C for 1 m, and 72 °C for 2 min) and then extension at 72 °C for 5 min. The *MsANS* fragment was amplified, subcloned into the pGEM T-easy vector, and then sequenced. The fragment was subsequently used to design gene-specific primers, which were used to clone the full-length cDNA of *MsANS* by rapid amplification of cDNA ends (RACE) technology.

We used a SMART RACE cDNA Amplification Kit (Clontech) to isolate the *MsANS* cDNA 3′ and 5′ ends. First, the 3′-RACE-ready and 5′-RACE-ready cDNA samples from *M. sprengeri* were prepared according to the manufacturer's protocol and then the 3′-RACE cDNA and 5′-RACE cDNA were used as templates for 3′-RACE and 5′-RACE, respectively. The *MsANS* cDNA 3′ end was amplified using 3′-gene-specific primers and the universal primers in the kit. For the first PCR amplification of 3′-RACE, MsANS-3 (5′-AATGCCCTCA GCCAGACCTA-3′) and UPM (Universal Primer Mix, Clontech) were used as the 3′-RACE primers, and 3′-RACE cDNA was used as the template. The *MsANS* cDNA5′ end was amplified using 5′-gene-specific primers and the universal primers in the kit. For PCR amplification of 5′-RACE, MsANS-4 (5′-AGCCCATCAAATCAACGACA-3′) and UPM were used as the PCR primers (5′-RACE), and 5′-RACE cDNA was used as the template. The PCR procedures were as follows: 25 cycles of 45 s at 94 °C, 45 s at 65 °C, and 1 min at 72 °C. Both ends of *MsANS* were obtained using 3′-RACE and 5′-RACE. The products were subcloned into the pGEM T-easy vector and then sequenced. The full-length cDNA sequence of *MsANS* was obtained by assembling the 3′-RACE, 5′-RACE, and core fragment sequences on ContigExpress (Vector NTI Suite 8.0). The open reading frame (ORF) of *MsANS* was predicted by the ORF Finder tool on the NCBI website (http://www.ncbi.nlm.nih.gov/gorf/

gorf.html). The full-length cDNA of *MsANS* was isolated by PCR amplification with the primer pair MsANS-5 (5′-ATCTTTCTTCACAAACACTAA-3′) and MsANS-6 (5′-CTTATT CGGATTTGAGGTTT-3′). The cycling conditions for PCR were as follows: 5 min at 94 °C, 36 cycles (1 min at 94 °C, 1 min at 50 °C, and 2 min at 72 °C), and 6 min at 72 °C. The amplified PCR product was purified, cloned into the pGEM T-easy vector, and then sequenced.

Bioinformatics Analysis

We used Clustal W, DNAman, and Mega 5.1 for multiple alignment analysis of the full-length ANS amino acid sequences and to construct the phylogenetic tree [32]. The protein secondary structure was predicted from the amino acid sequence using Self-Optimized Prediction Method from Alignment (SOPMA) [33]. ProtParam (www.expasy.org/tools/protparam.html) was used to analyze protein domains/functional sites, and ProtScale (www.expasy.ch/tools/protscale.html) was used to analyze the physicochemical characteristics and hydrophobicity of the putative protein [34]. Structural modeling based on sequence homology was performed using Swiss-Model [35], and the subcellular localization of the protein was predicted by Target P 1.1 [36].

qRT-PCR Analyses

To remove contaminating genomic DNA before cDNA synthesis, we treated the RNA with RNase-free DNAse I (Invitrogen) according to the manufacturer's instructions. Total RNA was quantified using a NanoDrop™ 1000 spectrophotometer before and after the DNAase I treatment, and its quality and integrity were checked by electrophoresis on agarose gels stained with EtBr. For quantitative real-time PCR (qRT-PCR), first-strand cDNA was synthesized using 2 μg total RNA in a volume of 20 μl using an SYBR PrimeScript RT-PCR Kit II (TaKaRa, Dalian, China) plus random hexamers and oligo(dT) primers. After reverse transcription, the reaction product was diluted 10-fold with sterile water. Real-time PCR was performed on an iQ5.0 instrument (Bio-Rad, Hercules, CA, USA) using an SYBR Green qPCR kit (TaKaRa) according to the manufacturer's instructions. The primer sequences for *MuANS1* and reference genes were as follows: MsANS-7, forward primer 5′-TGGCCATTCC CTCTCAATCTTTCTT-3′ and MsANS-8 reverse primer 5′- ACGCCGCCTTCTTCATATCC T-3′ (298-bp product); *Actin*, *Actin-1* forward-5′ ATCTGGCATCACACTTTCTACAATG-3″ and *Actin-2* reverse primer 5′ -CCAACCCAGGAGAAATGAACC-3′ (308-bp product); and *Polyubiquitin*, *pol-1* forward 5′ -GCAGCTTGAGGATGGCCGCACCCTC-3′ and *pol-1* reverse primer 5′ -AATCCGCAAGGGTCCTGCCATC-3′ (260-bp product). Each real-time PCR reaction consisted of a 20-μl reaction mixture containing 10 μM of each primer, 40 ng of cDNA, and 10 μl of SYBR Premix Ex Taq II. Thermal cycling conditions included an initial heat-denaturing step at 95 °C for 3 min, then 40 cycles of 95 °C for 20 s, 58 °C for 20 s, and 72 °C for 20 s. Fluorescence was measured at the end of each cycle. A melting curve analysis was performed by heating the PCR product from 58 to 95 °C. Transcript levels of *MuANS1* were normalized against that of *Actin* using the $2^{-\Delta\Delta CT}$ method. Values shown are means with standard deviations and were calculated from the results of three independent experiments.

HPLC Analysis of Anthocyanin in Flower Petals

M. sprengeri petal tissue (0.5 g) was ground in 1.5 mL 70 % methanol containing 2 % formic acid on ice. The mixture was then centrifuged at 10,000*g* for 10 min at 4 °C. The supernatant

was passed through a 0.22-μm syringe filter before HPLC analysis. Anthocyanins were analyzed using an Agilent 1100 HPLC equipped with a diode array detector (Agilent Technology), as described by Zhang et al. [37]. The total anthocyanin concentration was calculated based on a cyanidin-3-*O*-glucoside chloride standard (Sigma-Aldrich, St. Louis, MO, USA).

Results

Cloning of Full-Length cDNA of *MsANS*

A 584-bp PCR product was amplified using a pair of primers (*MsANS*-1 and *MsANS*-2). The fragment was then subcloned into the pGEM-T easy vector and sequenced. BLAST search results indicated that the 584-bp cDNA fragment showed homology to *ANS* genes from other plant species. Based on this information, the full-length cDNA sequence was obtained by RACE technology. The sequence was designated as *MsANS* (GenBank Accession No. KJ174325). The full-length *MsANS* is 1171-bp long (Supplemental Fig. 1) and contains a 1080-bp ORF encoding a 360 amino acid protein.

Bioinformatics Analysis

We conducted BLAST analyses in NCBI (http://blast.ncbi.nlm.nih.gov/Blast.cgi) and multi-alignment analyses using Clustal W and DNAman software and constructed a phylogenetic tree using Mega 5.1 software. In these analyses, MsANS showed high identity to ANS proteins from other species. MsANS showed an amino acid similarity of 74 % to the ANS from *Prunus salicina* var. *cordata* (gb|AEN19292.1|), 73 % to the ANS from *Pyrus communis* (gb|AGL50919.1|), 73 % to the ANS of *Prunus avium* (gb|ADZ54785.1|), and 74 % to the ANS of *Ampelopsis grossedentata* (gb|AGO02175.1|) (Fig. 1).

Using tools at Expasy (http://www.expasy.org), the theoretical molecular weight (MW) and isoelectric point (pI) of the deduced MsANS protein were predicted to 40.9 kDa and 5.15, respectively. The most abundant amino acid in MsANS is Glu (11.39 %) and the least abundant is Cys (0.83 %; Fig. 2a). The chemical formula of MsANS is $C_{1840}H_{2893}O_{539}S_{15}$. In total, the protein contains 58 negatively charged residues (Asp + Glu) and 43 positively charged residues (Arg + Lys). The grand average of hydropathicity (GRAVY) is −0.298, and the protein is hydrophobic (Fig. 2b). The SOPMA was used to predict the secondary structure of MsANS. The results indicated that MsANS consists of random coils (40.28 %), α-helices (36.39 %), extended strands (16.39 %), and β turns (6.94 %) (Fig. 2c). These structural characteristics indicate that MsANS is a member of the ANS family.

To further characterize MsANS, the three-dimensional structure was modeled using the Swiss Model (Fig. 2d). The protein consists of 11 α-helices and 10 β-sheets connected by random chains. A conserved domain search (http://www.ncbi.nlm.nih.gov/Structure/cdd/wrpsb.cgi) revealed that MsANS is a member of the 2-oxoglutarate (2OG)- and ferrous iron-dependent oxygenase family based on the presence of a 2OG-Fe(II)-oxy conserved domain. Protein subcellular positioning analysis by Target P 1.1 showed that the MsANS protein of 360 amino acids has low scores for chloroplast transit peptide (0.134) and mitochondrial targeting peptide (0.095), but high scores for secretory pathway signal peptide (0.436) and other parts of the leader peptide (0.419). Based on these results, MsANS synthesized in the nucleus may not be transported to chloroplasts and mitochondria, but the protein is secreted because it includes a signal peptide.

A

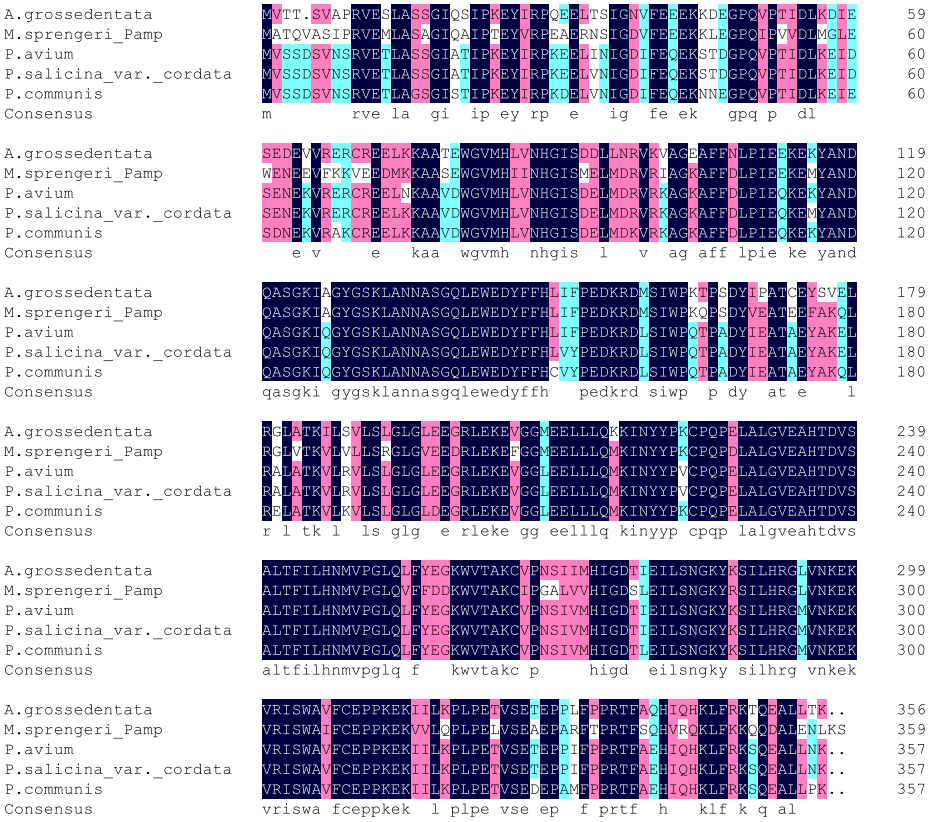

B

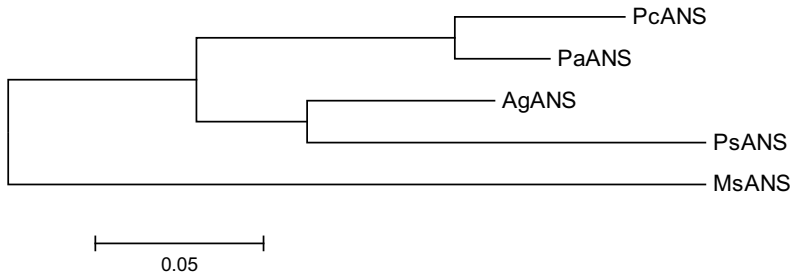

Fig. 1 Comparison of MsANS and its close homologs. **a** Comparison of amino acid sequences among ANS proteins. Conserved amino acids are indicated by the *dark shading*. *Pink* and *light blue* shading indicate X and X, respectively. **b** Phylogenetic tree of MsANS and its close homologs. *Scale bar* indicates genetic distance (*P. salicina* var. *cordata, M. sprengeri* Pamp., *P. avium*, *P. communis*, *M. domestica A. grossedentata*)

Anthocyanin Concentrations in Petals

We used HPLC to analyze the anthocyanin content in the petals from flowers of *M. sprengeri*. The main pigment was cyanidin-3-*O*-glucoside chloride (Fig. 3a–d). The highest concentration of this pigment was in red petals (3.4±0.08 mg/100 g) and the lowest was in the white petals

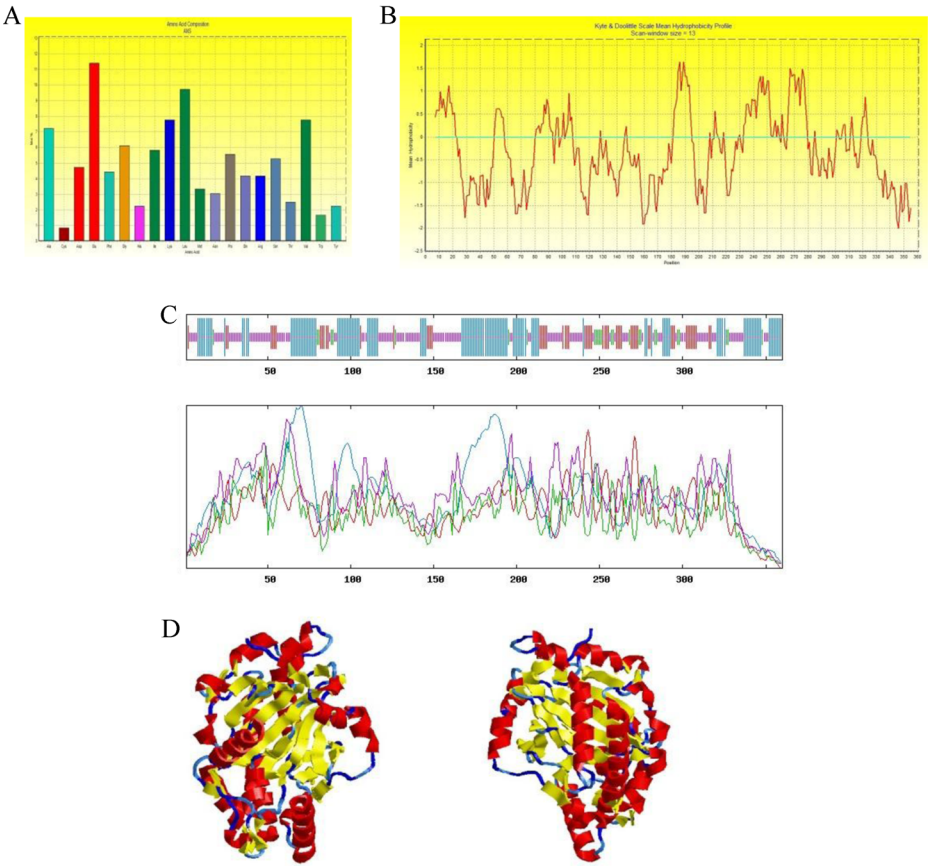

Fig. 2 Primary structure, secondary structure, and tertiary structure of MsANS protein of *M. sprengeri.* **a**, **b** Amino acid (AA) composition of MsANS of *M. sprengeri* (*left*) and predicted hydrophobic/hydrophilic regions in MsANS (*right*). **c** Predicted secondary structure of MsANS established by Self-Optimized Prediction Method from Alignment (SOPMA). Secondary structure of MsANS. α-Helix and extended strand are shown as *vertical long bars* and *vertical short bars*, respectively. *Horizontal line* represents random coil running through the whole molecule. Alpha helix (Hh): 131(36.39 %); 3_{10} helix (Gg): 0 (0.00 %); Pi helix (Ii): 0 (0.00 %); beta bridge (Bb): 0 (0.00 %); extended strand (Ee): 59 (16.39 %); beta turn (Tt): 25 (6.94 %); bend region (Ss): 0 (0.00 %); random coil (Cc): 145 (40.28 %); ambiguous states (?): 0 (0.00 %); other states: 0 (0.00 %). **d** Predicted tertiary structure of MsANS. α-Helices (11) are shown in *red*, β-sheets (10) in *yellow*, and strands in *blue*. Three-dimensional representations were created using RasTop (http://www.geneinfinity.org/rastop/)

(0.13±0.01 mg/100 g) (Fig. 4a). This is the first report that the main anthocyanin in flowers of *M. sprengeri* is cyanidin-3-*O*-glucoside chloride.

Transcript Profiles of *MsANS*

The transcript levels of *MsANS* in petals of M. *sprengeri* flowers of four different colors were analyzed by real-time quantitative PCR. The results showed that *MsANS* transcripts were present in petals of all colors, but the highest levels were in the red petals (Fig. 4b). The transcript level of *MsANS* was 26-fold higher in red petals than in white ones.

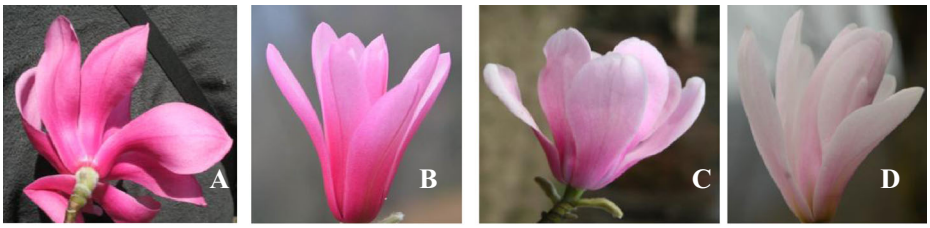

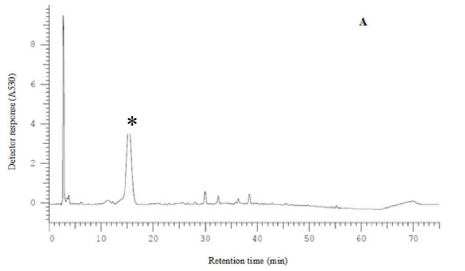

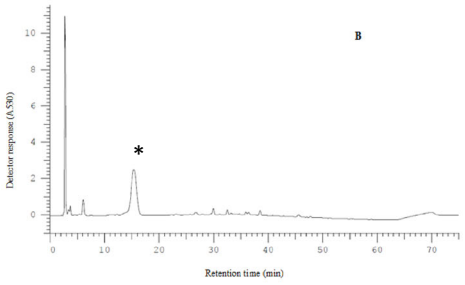

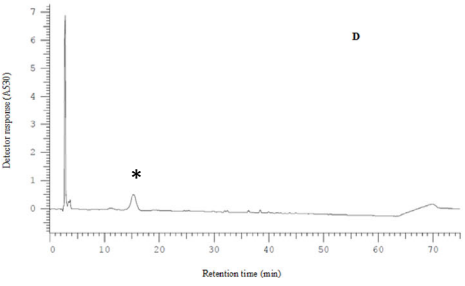

*Peak of cyanidin-3-o-glucoside chloride.

Fig. 3 Analysis of anthocyanin in *M. sprengeri* flowers of four different colors: *red* (**a**), *dark pink* (**b**), *light pink* (**c**), and *white* (**d**). Chromatograms corresponding to *A*, *B*, and *D* are shown. Peak in HPLC chromatograms was identified by comparing retention time with that of cyanidin-3-*o*-glucoside chloride standard. *Asterisk* peak of cyanidin-3-*o*-glucoside chloride

Discussion

In plants, ANS plays an important role in normal developmental processes and participates in adaptation to various environmental conditions. ANS proteins involved in anthocyanin biosynthesis have been identified in *Arabidopsis*, red cabbage, potato, *Brassica juncea*, tobacco,

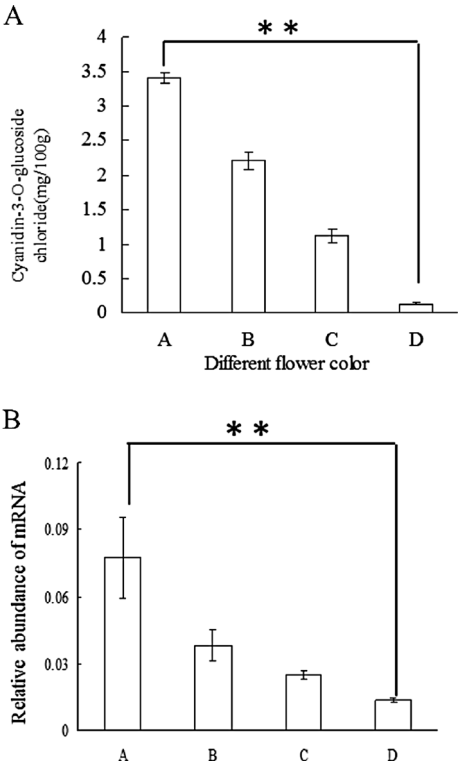

Fig. 4 Anthocyanin contents and transcript levels of *MsANS* in petals of *M. sprengeri* flowers of four different colors (see Fig. 3). **P<0.01 (indicates significant difference, *t* test). Experiments were repeated at least three times. **a** Anthocyanin content in petals of flowers of four different colors. Anthocyanin concentrations were determined by HPLC with cyanidin-3-*o*-glucoside chloride as the standard. Values shown are mean±SD (n=3). **b** Transcript levels of *MsANS* in petals of flowers of four different colors. Transcript levels of *MsANS* were normalized to that of *Actin*. Values shown are mean±SE (*bars*) of three independent experiments per time point

grape, and peach [38–43], but there are few reports on ANS proteins in *Magnolia*. In this study, we isolated the full-length cDNA of *MsANS* from *M. sprengeri*. The gene was found to be 1171 bp long with a 1080-bp ORF encoding a 360 amino acid protein. Nucleotide BLAST-X analyses revealed that the cloned cDNA sequence of *MsANS* shows high similarity to ANS genes from other species. Multiple alignment and phylogenetic tree analyses showed that the deduced sequence of MsANS shows high identity with ANS proteins from other plant species. A bioinformatics analysis showed that MsANS contains 11 α-helices and 10 β-sheets. Based on the presence of a 2OG-Fe(II)-oxy conserved domain, this enzyme is a member of the 2OG- and Fe(II)-dependent oxygenase family. MsANS catalyzes the penultimate step in anthocyanin biosynthesis [44, 45]. The sequence similarities between ANSs and other flavonoid 2OG-dependent deoxygenases imply that MsANS might have the same catalytic function as that of other ANSs.

The flowers of *M. sprengeri* show diverse colors and contain polyphenolic compounds; therefore, this species is becoming an excellent model plant to study the mechanisms of pigmentation. In nature, the color of *M. sprengeri* flowers varies from white to red, but the molecular mechanism of the formation of the red color remains unclear. In plants, the petal color is mainly a result of the accumulation of anthocyanins [17, 46–48], which are major

pigments with a wide range of colors. Thus, we focused on anthocyanin biosynthesis and its regulation in *M. sprengeri* petals.

The results of HPLC analysis showed that cyanidin-3-*O*-glucoside chloride is the main pigment in petals in *M. sprengeri*. To our knowledge, this is the first report to identify the pigment in flowers of *M. sprengeri*. Several biosynthetic enzymes, including ANS, play key roles in anthocyanin biosynthesis. In previous studies, *ANS* transcripts have been detected in various tissues of diverse plants [49–51]. There were reports that *ANS* transcript levels are higher in the skin of grape berries [52], the flesh of *Raphanus sativus* [53], and the flowers of tartary buckwheat [54]. In this study, we investigated the transcript levels of *MsANS* in the petals of magnolia flowers of four different colors. As expected, the transcript levels of *MsANS* were lower in the white petals than in the red petals. This result suggested that a higher expression level of anthocyanin biosynthesis genes in red petals could be the reason for their deep red color. There was a low anthocyanin content in the white petals. It is possible that transcription factor(s), for example, MYB, bHLH, and WD40, regulate the expression of several structural anthocyanin genes in *M. sprengeri*, including *ANS*, to control anthocyanin accumulation in the flowers.

Conclusions

Our results show that MsANS is structurally conserved and that post-transcriptional RNA processing may be involved in controlling flower color variations. Although we have not yet fully described the function of MsANS, our results suggest that this protein is active in coloration because there were higher transcript levels of *MsANS* in red petals than in white petals. In future studies, it will be important to further evaluate the regulation and function of MsANS in *Magnolia*. The isolation and characterization of this gene are important steps in the molecular breeding of *Magnolia*.

Acknowledgments This work was supported by the National Forestry Research and Special Public Service Sectors (200904004).

References

1. Kang, Y. X., & Ejder, E. (2011). *Magnolia sprengeri* Pamp.: morphological variation and geographical distribution. *Plant Biosystems, 145*, 906–923.
2. Weiss, D. (2000). Regulation of flower pigmentation and growth: multiple signaling pathways control anthocyanin synthesis in expanding petals. *Physiologia Plantarum, 110*, 152–157.
3. Zhang, Q., Su, L. J., Chen, J. W., Zeng, X. Q., Sun, B. Y., & Peng, C. L. (2012). The antioxidative role of anthocyanins in *Arabidopsis* under high-irradiance. *Biologia Plantarum, 56*, 97–104.
4. Cerezo, A. B., Cuevas, E., Winterhalter, P., Garcia-Parrilla, M. C., & Troncoso, A. M. (2010). Isolation, identification, and antioxidant activity of anthocyanin compounds in Camarosa strawberry. *Food Chemistry, 123*, 574–582.
5. Grotewold. (2006). The genetics and biochemistry of floral pigments. *Annual Review of Plant Biology, 7*, 761–780.
6. Reque, P. M., Steffens, R. S., Jablonski, A., Flores, S. H., de Rios, A. O., & de Jong, E. V. (2014). Cold storage of blueberry (*Vaccinium* spp.) fruits and juice: anthocyanin stability and antioxidant activity. *Journal of Food Composition and Analysis, 33*, 111–116.
7. Qiu, J., Sun, S., Luo, S., Zhang, J., Xiao, X., Zhang, L., Wang, F., Liu, S. (2014). Arabidopsis *AtPAP1* transcription factor induces anthocyanin production in transgenic T*araxacum brevicorniculatum. Plant Cell Reports*.

8. Ross, J. A., & Kasum, C. M. (2002). Dietary flavonoids: bioavailability, metabolic effects, and safety. *Annual Review of Nutrition, 22*, 19–34.
9. Katsuben, N., Washitak, I., & Sushidat, T. (2003). Induction of apoptosis in cancer cells by Bilberry (*Vaccinium myrtillus*) and the Anthocyanins. *Journal of Agricultural and Food Chemistry, 51*, 68–75.
10. Kruger, M. J., Davies, N., Myburgh, K. H., & Lecour, S. (2014). Proanthocyanins, anthocyanins and cardiovascular diseases. *Food Research International, 59*, 41–52.
11. Mazza, G. J. (2007). Anthocyanins and heart health. *Annali dell Istituto Superiore di Sanita, 43*(4), 369–374.
12. Irani, N., & Grotewold, E. (2005). Light-induced morphological alteration in anthocyanin-accumulating vacuoles of maize cells. *BMC Plant Biology, 5*, 7.
13. Feng, F. J., Li, M. J., Ma, F. W., & Chen, L. L. (2013). Phenylpropanoid metabolites and expression of key genes involved in anthocyanin biosynthesis in the shaded peel of apple fruit in response to sun exposure. *Plant Physiology and Biochemistry, 69*, 54–61.
14. Ithal, N., & Reddy, A. R. (2004). Rice flavonoid pathway genes, OsDfr and OsAns, are induced by dehydration, high salt and ABA, and contain stress responsive promoter elements that interact with the transcription activator, OsC1-MYB. *Plant Science, 166*, 1505–1513.
15. Koes, R. E., Quattrocchio, F., & Mol, J. N. M. (1994). The flavonoid biosynthetic pathway in plants: function and evolution. *Bioessays, 16*, 123–132.
16. Holton, T. A., & Cornish, E. C. (1999). Genetics and biochemistry of anthocyanin biosynthesis. *Plant Cell, 7*, 1071–1083.
17. Winkel-Shirley, B. (2001). Flavonoid biosynthesis: a colorful model for genetics, biochemistry, cell biology, and biotechnology. *Plant Physiology, 126*, 485–493.
18. Koes, R., Verweij, W., & Quattrocchio, F. (2005). Flavonoids: a colorful model for the regulation and evolution of biochemical pathways. *Trends in Plant Science, 10*, 236–242.
19. Chen, S. M., Li, C. H., Zhu, X. R., Deng, Y. M., Sun, W., Wang, L. S., Chen, F. D., & Zhang, Z. (2012). The identification of flavonoids and the expression of genes of anthocyanin biosynthesis in the chrysanthemum flowers. *Biologia Plantarum, 56*, 458–464.
20. Huang, W., Sun, W., & Wang, Y. (2012). Isolation and molecular characterisation of flavonoid 3′-hydroxylase and flavonoid 3′5′-hydroxylase genes from a traditional Chinese medicinal plant, *Epimedium sagittatum. Gene, 497*, 125–130.
21. Nakajima, J., Tanaka, Y., Yamazaki, M., & Saito, K. (2001). Reaction mechanism from leucoanthocyanidin to anthocyanidin 3-glucoside, a key reaction for coloring in anthocyanin biosynthesis. *Journal of Biological Chemistry, 276*, 25797–25803.
22. Yuan, Y., Ma, X. H., Shi, Y. M., & Tang, D. Q. (2013). Isolation and expression analysis of six putative structural genes involved in anthocyanin biosynthesis in *Tulipa fosteriana. Scientia Horticulturae, 153*, 93–102.
23. Zhou, W., Huang, C. T., Gong, Y. F., Feng, Q. L., & Gao, F. (2010). Molecular cloning and expression analysis of an A*NS* gene encoding anthocyanidin synthase from purple-fleshed sweet potato [*Ipomoea batatas* (L.) Lam]. *Plant Molecular Biology Reporter, 28*, 112–121.
24. Gong, Z., Yamazaki, M., Sugiyama, M., Tanaka, Y., & Saito, K. (1997). Cloning and molecular analysis of structural genes involved in anthocyanin biosynthesis and expressed in a forma-specific manner in *Perilla frutescens. Plant Molecular Biology, 35*, 915–927.
25. Saito, K., Kobayashi, M., Gong, Z., Tanaka, Y., & Yamazaki, M. (1999). Direct evidence for anthocyanidin synthase as a 2-oxoglutaratedependent oxygenase: molecular cloning and functional expression of cDNA from a red forma of Perilla frutescens. *Plant Journal, 17*, 181–189.
26. Ramsay, N. A., Walker, A. R., Mooney, M., & Gray, J. C. (2003). Two basic-helix-loop-helix genes (MYC-146 and GL3) from Arabidopsis can activate anthocyanin biosynthesis in a white-flowered *Matthiola incana* mutant. *Plant Molecular Biology, 52*, 679–688.
27. Bogs, J., Jaffé, F. W., Takos, A. M., Walker, A. R., & Robinson, S. P. (2007). The grapevine transcription factor VvMYBPA1 regulates proanthocyanidin synthesis during fruit development. *Plant Physiology, 143*, 1347–1361.
28. Dubos, C., Le Gourrierec, J., Baudry, A., Huep, G., Lanet, E., Debeaujon, I., Routaboul, J. M., Alboresi, A., Weisshaar, B., & Lepiniec, L. (2008). MYBL2 is a new regulator of flavonoid biosynthesis in *Arabidopsis thaliana. Plant Journal, 55*, 940–953.
29. Gonzalez, A., Zhao, M., Leavitt, J. M., & Lloyd, A. M. (2008). Regulation of the anthocyanin biosynthetic pathway by the TTG1/bHLH/Myb transcriptional complex in *Arabidopsis* seedlings. *Plant Journal, 53*, 814–827.
30. Peel, G. J., Pang, Y., Modolo, L. V., & Dixon, R. A. (2009). The LAP1 MYB transcription factor orchestrates anthocyanidin biosynthesis and glycosylation in Medicago. *Plant Journal, 59*, 136–149.
31. Zhou, L. L., Shi, M. Z., & Xie, D. Y. (2012). Regulation of anthocyanin biosynthesis by nitrogen in TTG1–GL3/TT8–PAP1-programmed red cells of *Arabidopsis thaliana. Planta, 236*, 825–837.

32. Thompson, J. D., Higgins, D. G., & Gibson, T. J. (1994). CLUSTAL W: improving the sensitivity of progressive multiple sequence alignment through sequence weighting, positions-specific gap penalties and weight matrix choice. *Nucleic Acids Research, 22*, 4673–4680.
33. Geourjon, C., & Deléage, G. (1995). SOPMA: significant improvement in protein secondary structure prediction by consensus prediction from multiple alignments. *Cabios, 11*, 681–684.
34. Gasteiger, E., Hoogland, C., Gattiker, A., Duvaud, S., Wilkins, M. R., Appel, R. D., & Bairoch, A. (2005). In J. M. Walker (Ed.), *Protein identification and analysis tools on the ExPASyServer* (pp. 571–607). The Proteomics Protocols Handbook: Humana Press.
35. Guex, N., & Peitsch, M. C. (1997). SWISS-MODEL and the Swiss-Pdb Viewer: an environment for comparative protein modeling. *Electrophoresis, 18*, 2714–2723.
36. Emanuelsson, O., Nielsen, H., Brunak, S., & von Heijne, G. (2000). Predicting subcellular localization of proteins based on their N-terminal amino acid sequence. *Journal of Molecular Biology, 300*(4), 1005–1016.
37. Zhang, Y. Z., Li, P. M., & Cheng, L. L. (2010). Developmental changes of carbohydrates, organic acids, amino acids, and phenolic compounds in 'Honeycrisp' apple flesh. *Food Chemistry, 123*, 1013–1018.
38. Yan, M. L., Liu, X. J., Guan, C. Y., Chen, X. B., & Liu, Z. S. (2011). Cloning and expression analysis of an anthocyanidin synthase gene homolog from *Brassica juncea*. *Molecular Breeding, 28*, 313–322.
39. Wang, H. L., Wang, W., Zhang, P., Pan, Q. H., Zhan, J. C., & Huang, W. D. (2010). Gene transcript accumulation, tissue and subcellular localization of anthocyanidin synthase (ANS) in developing grape berries. *Plant Science, 179*, 103–113.
40. Keifenheim, D. L., Smith, A. G., & Tong, C. B. S. (2006). Cloning and accumulation of anthocyanin biosynthesis genes in developing tubers. *American Journal of Potato Research, 83*, 233–239.
41. Yuan, Y. X., Chiu, L. W., & Li, L. (2009). Transcriptional regulation of anthocyanin biosynthesis in red cabbage. *Planta, 230*, 1141–1153.
42. Shi, M. Z., & Xie, D. Y. (2010). Features of anthocyanin biosynthesis in *pap1-D* and wild-type *Arabidopsis thaliana* plants grown in different light intensity and culture media conditions. *Planta, 231*, 1385–1400.
43. Lim, S. H., Kim, J. K., Lee, J. Y., Kim, Y. M., Sohn, S. H., Kim, D. H., & Ha, S. H. (2013). Petal-specific activity of the promoter of an anthocyanidin synthase gene of tobacco (*Nicotiana tabacum* L.). *Plant Cell, Tissue and Organ Culture, 114*, 373–383.
44. Turnbull, J. J., Nakajima, J., Welford, R. W., Yamazaki, M., Saito, K., & Schofield, C. J. (2004). Mechanistic studies on three 2-oxoglutarate-dependent oxygenases of flavonoid biosynthesis: anthocyanidin synthase, flavonol synthase, and flavanone 3 betahydroxylase. *Journal of Biological Chemistry, 279*, 1206–1216.
45. Wilmouth, R. C., Turnbull, J. J., Welford, R. W., Clifton, I. J., Prescott, A. G., & Schofield, C. J. (2002). Structure and mechanism of anthocyanidin synthase from Arabidopsis thaliana. *Structure, 10*, 93–103.
46. Yamagishi, M., Kishimoto, S., & Nakayama, M. (2010). Carotenoid composition and changes in expression of carotenoid biosynthetic genes in tepals of Asiatic hybrid lily. *Plant Breeding, 129*, 100–107.
47. Lightbourn, G. J., Griesbach, R. J., Novotny, J. A., Clevidence, B. A., Rao, D. D., & Stommel, J. R. (2008). Effects of anthocyanin and carotenoid combinations on foliage andimmature fruit color of Capsicum *annuum L. Journal of Heredity, 99*, 105–111.
48. Holton, T. A., & Cornish, E. C. (1995). Genetics and biochemistry of anthocyanin biosynthesis. *Plant Cell, 7*, 1071–1083.
49. Wang, Y. S., Gao, L. P., Shan, Y., Liu, Y. J., Tian, Y. W., & Xia, T. (2012). Influence of shade on flavonoid biosynthesis in tea *Camellia sinensis* (L.). *Scientia Horticulturae, 141*, 7–16.
50. Rosati, C., Cadic, A., Duron, M., Ingouff, M., & Simoneau, P. (1999). Molecular characterization of the anthocyanidin synthase gene in *Forsythia× intermedia* reveals organ-specific expression during flower development. *Plant Science, 149*, 73–79.
51. Wang, H., Wang, W., Li, H., Zhang, P., Zhan, J., & Huang, W. (2011). Expression and tissue and subcellular localization of anthocyanidin synthase (ANS) in grapevine. *Protoplasma, 248*, 267–279.
52. Xu, F., Cheng, H., Cai, R., Li, L. L., Chang, J., Zhu, J., Zhang, F. X., Chen, L. J., Wang, Y., Cheng, S. H., & Cheng, S. Y. (2008). Molecular cloning and function analysis of an anthocyanidin synthase gene from *Ginkgo biloba*, and its expression in abiotic stress responses. *Molecules and Cells, 26*, 536–547.
53. Park, N. I., Xu, H., Li, X., Jang, I. H., Park, S., Ahn, G. H., Lim, Y. P., Kim, S. J., & Park, S. U. (2011). Anthocyanin accumulation and expression of anthocyanin biosynthetic genes in Radish (*Raphanus sativus*). *Journal of Agricultural and Food Chemistry, 59*, 6034–6039.
54. Park, N. J., Li, X., Suzuki, T., Woo, S. H., Park, C. H., & Park, S. U. (2011). Differential expression of anthocyanin biosynthetic genes and anthocyanin accumulation in tartary buckwheat cultivars 'Hokkai t8' and 'Hokkai t 10'. *Journal of Agricultural and Food Chemistry, 59*, 2356–2361.